LETTERS
PUBLISHED ONLINE: 23 OCTOBER 2011 | DOI: 10.1038/NNANO.2011.184
nature nanotechnology

Skin-like pressure and strain sensors based on transparent elastic films of carbon nanotubes

Darren J. Lipomi[1†], Michael Vosgueritchian[1†], Benjamin C-K. Tee[2†], Sondra L. Hellstrom[3], Jennifer A. Lee[1], Courtney H. Fox[1] and Zhenan Bao[1*]

Transparent, elastic conductors are essential components of electronic and optoelectronic devices that facilitate human interaction and biofeedback, such as interactive electronics[1], implantable medical devices[2] and robotic systems with human-like sensing capabilities[3]. The availability of conducting thin films with these properties could lead to the development of skin-like sensors[4] that stretch reversibly, sense pressure (not just touch), bend into hairpin turns, integrate with collapsible, stretchable and mechanically robust displays[5] and solar cells[6], and also wrap around non-planar and biological[7–9] surfaces such as skin[10] and organs[11], without wrinkling. We report transparent, conducting spray-deposited films of single-walled carbon nanotubes that can be rendered stretchable by applying strain along each axis, and then releasing this strain. This process produces spring-like structures in the nanotubes that accommodate strains of up to 150% and demonstrate conductivities as high as 2,200 S cm^{-1} in the stretched state. We also use the nanotube films as electrodes in arrays of transparent, stretchable capacitors, which behave as pressure and strain sensors.

Metallic films on elastomeric substrates can accommodate strain by means of controlled fracture[12] or buckling[13], but they are generally opaque. Conductive polymers can be buckled to form stretchable transparent electrodes[6,14], but topographic buckles may be incompatible with devices that require planar interfaces. Films of carbon nanotubes[15] and graphene[16] are candidates for stretchable, transparent electrodes because (1) the long mean-free path of electrons in defect-free films produces high conductivity, without decreasing the transparency[17], and (2) networks of nanotubes and graphene sheets permit some elasticity without destroying the contiguity of the film. One collaboration[16,18] has produced graphene sheets with values of transparency T and sheet resistance R_s approaching those of tin-doped indium oxide (ITO), but the resistance increased by an order of magnitude when strained by 30% (ref. 16). Others have demonstrated uniaxial stretchability in highly aligned films of nanotubes pulled from vertical forests[19]. There have also been reports of films of nanotubes that can be stretched by up to 100% along the axis of aligned nanotubes without a significant change in resistance[15]. Randomly deposited films of nanotubes have been stretched up to 700%, but the resistance increased by an order of magnitude following the application of $\leq$50% strain[20]. Recently, researchers reported a transparent nanotube film embedded in an elastomer for stretchable organic light-emitting devices; the resistance of the most conductive film (50 Ω sq^{-1} at $T = 63\%$) increased by 100% at 50% strain[21]. Stretchable, opaque networks of conductive particles demonstrated thus far include a nanotube–fluoroelastomer composite with conductivity of 9.7 S cm^{-1} at 118% strain[5], a nanotube–silver composite material with 20 S cm^{-1} at 140% (ref. 22) and buckled nanotube films with 900 S cm^{-1} at 40% (ref. 23). Combining high conductivity ($\sigma > 100$ S cm^{-1}) and transparency (>80%) at high strain ($\varepsilon \geq 150\%$) remains a challenge.

We produced conductive, transparent, stretchable nanotube films by spray-coating (nanotube length = 2–3 μm)[24,25] directly onto a substrate of poly(dimethylsiloxane) (PDMS, activated by exposure to ultraviolet/O_3) from a solution in *N*-methylpyrrolidone. We obtained the best values of R_s and σ by spin-coating a solution of charge-transfer dopant (tetrafluorotetracyanoquinodimethane (F4TCNQ) in chloroform) over the films[26]. Doped and undoped films exhibited similar electromechanical behaviour. We obtained values of $R_s = 328\ \Omega$ sq^{-1} and $T = 79\%$, and maximum values of $\sigma = 1{,}100$ S cm^{-1} for a 100 nm film with $T = 68\%$, at 0% strain. (See Supplementary Fig. S1 for the measurement of film thickness.)

Figure 1a presents the evolution of the change in resistance ($\Delta R/R_0$) as a function of strain for seven stages of applied strain and relaxation: $0 \rightarrow 50\% \rightarrow 0\% \rightarrow 100\% \rightarrow 0\% \rightarrow 150\% \rightarrow 0\% \rightarrow 200\%$. With the first application of 50% strain, R increased by 0.71. We attribute this increase to irrecoverable loss of junctions between nanotubes. When we returned the film to 0% strain, $\Delta R/R_0$ decreased to 0.64 (as opposed to 0, its original value). Following the application of 100% strain, the resistance retraced itself until it reached 50% (the previous maximum strain), after which the slope of $\Delta R/R_0$ increased. We observed similar behaviour when we relaxed the film on reaching $\varepsilon = 100\%$ and 150%. At $\varepsilon \approx 170\%$, the resistance of the film increased irreversibly by several orders of magnitude. We estimate a lower limit on conductivity at 150% strain of 2,200 S cm^{-1} (see Supplementary Information for a discussion of conductivity under strain).

The effect of strain history on resistance implies that these nanotube films can be 'programmed' by the first cycle of strain and release, to be reversibly stretchable within the range defined by the first strain. Figure 1b shows four cycles of strain from 0 to 50%, in which the resistance increases reversibly by $\leq$10% because the film was previously strained to a maximum of 50%. Measurement of R over the course of 12,500 cycles of stretching produced the plot shown in Fig. 1c. Over the course of this experiment, the resistance had decreased by 22% at the 1,500th cycle, and then increased linearly. We observed the same minimum in resistance at ~1,000 cycles of stretching in three similar experiments. We attribute the minimum in resistance to a period in which the nanotube bundles adopted their optimum morphology. Subsequent cycles of stretching possibly decreased the number of conductive junctions between bundles.

[1]Department of Chemical Engineering, Stanford University, Stanford, California 94305, USA, [2]Department of Electrical Engineering, Stanford University, Stanford, California 94305, USA, [3]Department of Applied Physics, Stanford University, Stanford, California 94305, USA; [†]These authors contributed equally to this work. *e-mail: zbao@stanford.edu

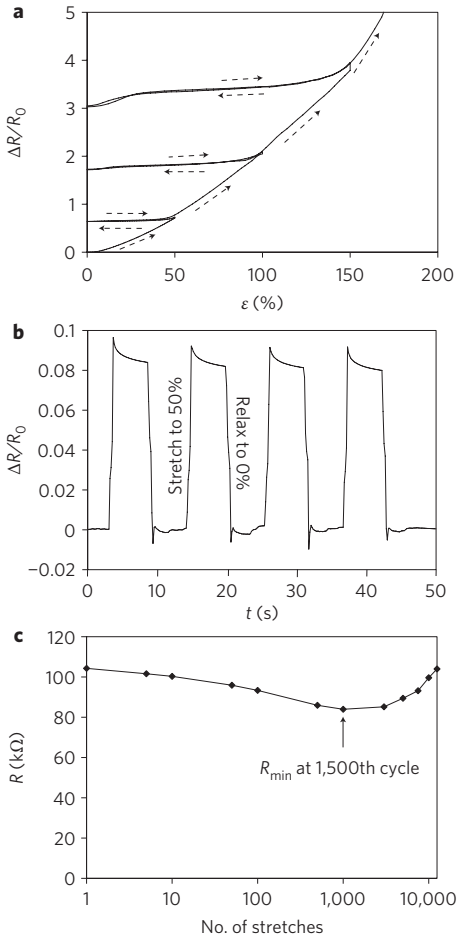

Figure 1 | Effects of applied strain on films of spray-coated carbon nanotubes on PDMS substrates. a, Change in resistance $\Delta R/R_0$ versus strain ε for a nanotube film on a PDMS substrate. When the film is strained (arrow, bottom left), $\Delta R/R_0$ increases, and remains constant as the strain is released. When the strain is increased again, $\Delta R/R_0$ remains constant, and then increases when ε exceeds the value at which the strain was released before. This sequence is repeated up to $\Delta R/R_0 \approx 5$ and $\varepsilon \approx 150\%$. **b**, $\Delta R/R_0$ versus time in response to four cycles of stretching from 0 to 50%. **c**, Resistance versus number of stretches (on a log scale) over 12,500 cycles of stretching to 25%.

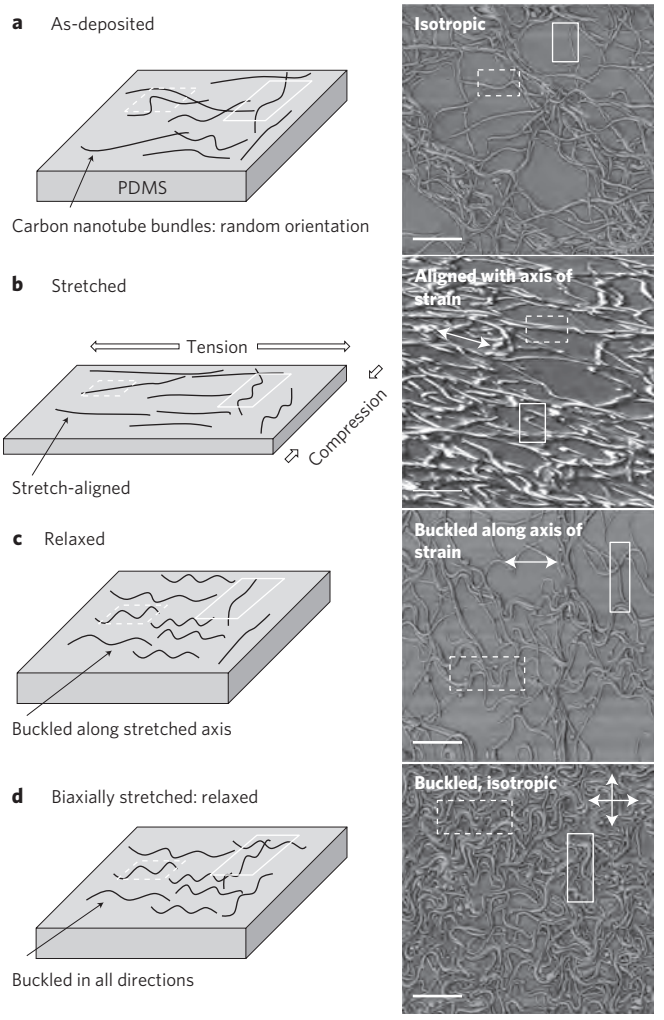

Figure 2 | Evolution of morphology of films of carbon nanotubes with stretching. Schematics (left) and corresponding AFM phase images (right) of nanotube films as deposited (**a**), under strain (**b**), stretched and released along one axis (**c**), and stretched and released along two axes (**d**). The bundles are considerably longer than the individual nanotubes within them. Dashed and solid white boxes highlight the bundles of nanotubes buckled along the horizontal and vertical axes, respectively. Scale bars, 600 nm.

We examined the morphology of the nanotube films using atomic force microscopy (AFM) to understand why the resistance of the film was a function of its strain history. Figure 2 shows a series of schematic diagrams depicting the change in morphology of nanotubes on a PDMS substrate with strain, as well as corresponding AFM images. The 'as-deposited' film (Fig. 2a) exhibited bundles (diameter, 10–20 nm) of nanotubes with isotropic orientations. Activation of the surface with ultraviolet/O_3 before deposition was critical, because the nanotube bundles formed large, sparse aggregates non-uniformly on hydrophobic substrates. Figure 2b shows an AFM image of the nanotube film under strain. The application of strain exerted tensile stress on bundles with components oriented with the axis of strain and aligned them to it (Fig. 2b, dashed box). Compressive stress (due to the Poisson effect) on bundles oriented perpendicular to the axis of strain caused them to buckle in plane into waves (Fig. 2b, solid box). After stretching the film for the first time, relaxation to 0% strain produced waves in the bundles that had been aligned by stretching (Fig. 2c). The amplitude of waves increased with the initial strain (Supplementary Fig. S2). Other researchers have observed a different, although similar, phenomenon, with the buckling of individual nanotubes (as opposed to bundles) on the surface of PDMS under small compressive strains of 5% (as opposed to 150%), with buckling amplitudes <10 nm and perpendicular (as opposed to parallel) to the plane of the substrate[27].

The stretch-induced change in the morphology of the uniaxially stretched films produced unequal conductivities along the stretched and unstretched axes. When both axes were stretched and released, all nanotube bundles exhibited buckling, but the orientations were random (Fig. 2d), and the resistance was the same along the stretched and unstretched axes. Biaxially stretched films were reversibly stretchable in any direction (see Supplementary Information and Fig. S3).

The technological goal is to integrate these stretchable, transparent conductors into interactive optoelectronic devices and sensors for biofeedback. We therefore fabricated transparent and stretchable parallel-plate capacitors that could manifest changes in pressure and strain as changes in capacitance (Fig. 3a). The devices comprised two strips of PDMS bearing stretchable nanotube films, which we laminated together, face-to-face, with Ecoflex silicone elastomer. Ecoflex (Shore hardness 00-10) is more easily

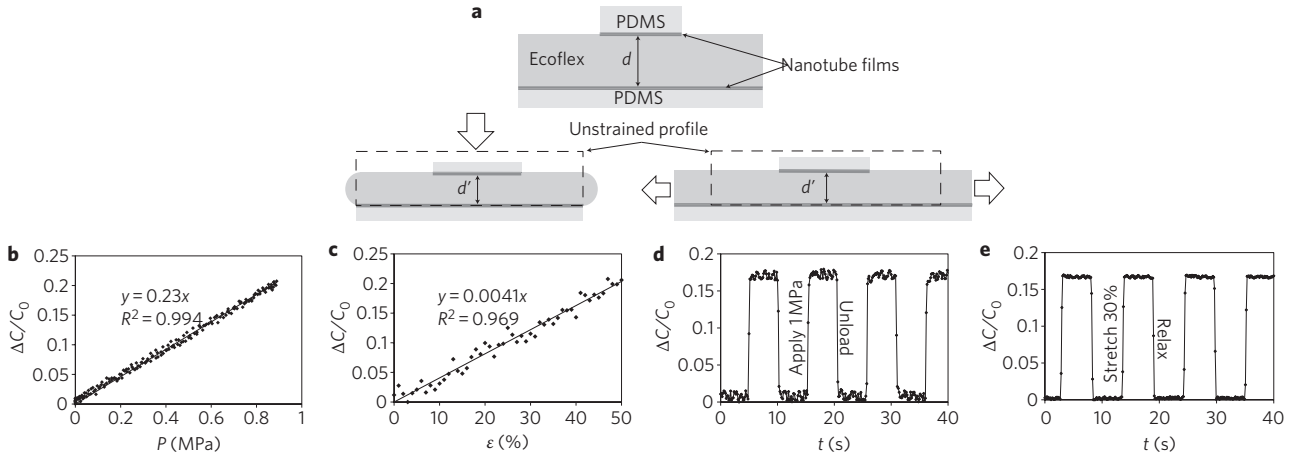

Figure 3 | Use of stretchable nanotube films in compressible capacitors that can sense pressure and strain. a, Schematic showing a stretchable capacitor with transparent electrode (top), and the same capacitor after being placed under pressure (left) and being stretched (right). **b**,**c**, Change in capacitance $\Delta C/C_0$ versus pressure P (**b**) and strain ε (**e**). **d**,**e**, $\Delta C/C_0$ versus time t over four cycles of applied pressure (**d**) and stretching (**e**).

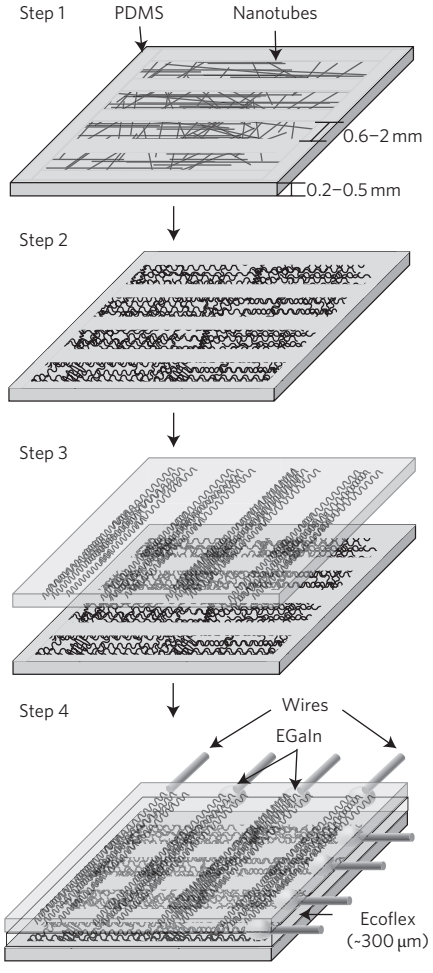

Figure 4 | Summary of processes used to fabricate arrays of transparent, compressible, capacitive sensors. Spray-coating through a stencil mask produces lines of randomly oriented nanotubes (step 1). A one-time application of strain and release produces waves in the direction of strain (step 2). A second patterned substrate is positioned (face to face) over the first (step 3). The two substrates are bonded together using Ecoflex silicone elastomer, which, when cured, serves as a compressible dielectric layer (step 4). Drops of a liquid metal, EGaIn, make conformal contact with the termini of the nanotube electrodes and are embedded within the device. Copper nanowires connect the device to an LCR meter in the laboratory.

deformed than PDMS (Shore hardness A-48)[28]. The capacitance of a parallel-plate capacitor is proportional to $1/d$, where d is the spacing between plates. Application of pressure (Fig. 3a (left), b,d) and tensile strain (Fig. 3a (right), c, e) both resulted in a shortened distance between the electrodes (d'). Capacitance C is linearly dependent on pressure to 1 MPa (Fig. 3b) and strain to 50% (Fig. 3c) over the ranges tested. The smallest change in capacitance distinguishable from noise was ~50 kPa. The figure of merit of conventional strain gauges is the gauge factor, $(\Delta R/R_0)/\varepsilon$ (ref. 29). We can also define a capacitive gauge factor, $(\Delta C/C_0)/\varepsilon$, which is the slope of the linear fit in Fig. 3c (see Supplementary Information for discussion); in this case we determined $(\Delta C/C_0)/\varepsilon$ to be 0.004. Figure 3d shows capacitance versus time for four cycles of applied pressure using an electrically insulating tip to apply the load. Figure 3e shows a similar plot of capacitance versus time over four cycles of stretching to 30%. The timescale over which the pixels recovered was smaller than that over which our instruments could load and unload the sample, $\leq$125 ms.

We next fabricated a grid of capacitors to produce a device that had spatial resolution (Fig. 4). We began by depositing nanotube lines through a PDMS membrane that contained apertures (step 1)[30]. Applying strain rendered the film reversibly stretchable (step 2). We positioned a second patterned substrate orthogonal to the first (step 3), placed liquid eutectic gallium-indium (EGaIn)[28,31,32] and copper wires at the ends of the nanotube lines, and laminated the substrates together with Ecoflex (step 4).

We formed patterns of nanotube films with linewidths of 0.6–2 mm and pitches of 2–4 mm. We generated arrays of 4–64 capacitors ('pixels') with areas of 0.4–4 mm^2 and pitches of 2–4 mm. The thickness of the Ecoflex layer was ~300 μm. Figure 5a,b shows the largest array we fabricated: an 8 × 8 array of nanotube lines, with width and spacing of 2 mm. The average capacitance of each pixel was 13.3 ± 1.4 pF ($N = 64$). Transparency of the nanotube lines varied across the substrate from 88 to 95%.

In principle, changes in capacitance due to strain could be distinguished from those due to pressure. Tensile straining would affect pixels along the axis of strain; pressure would affect the pixels in the immediate vicinity of the load. We found that the crosstalk between adjacent pixels in the 64-pixel device was low, and the change in capacitance registered by the pixel on which pressure was applied was five times higher than the average of that registered by the four adjacent pixels (Fig. 5c). This observation highlights the advantages of using stretchable materials for pressure sensors, for which the greatest compression occurs at the site of the load. The crosstalk for devices fabricated on a

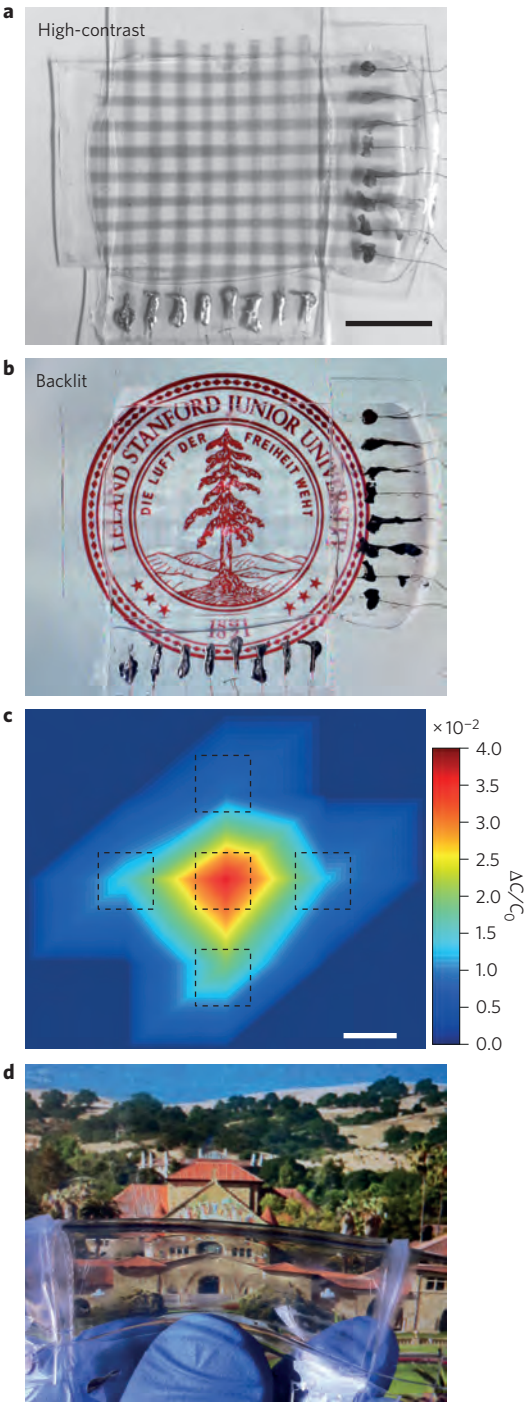

Figure 5 | Images showing the characteristics of a 64-pixel array of compressible pressure sensors. a, Photograph of the device, with enhanced contrast to show the lines of nanotubes (scale bar, 1 cm). **b**, Photograph of the same device reversibly adhered to a backlit liquid-crystal display. **c**, Map of the estimated pressure profile over a two-dimensional area based on the change in capacitance registered by a central pixel and its four nearest neighbours when a pressure of 1 MPa is applied to the central pixel (scale bar, 2 mm). **d**, Image of the device being deformed by hand.

non-stretchable polyester substrate was approximately two times greater than that of the present device, as determined by the relative increase in capacitance measured in pixels 4 mm from the site of the load[33].

Our device is less sensitive than another 'skin-like' device reported in the literature[33], but there are currently no other devices that are both transparent and stretchable, and few have demonstrated the ability to detect both pressure and strain[4]. One device has been demonstrated based on nanowire field-effect transistors that could detect a few kilopascals[34], whereas another device with the geometry of a fishnet could undergo tensile deformations while detecting pressures on the order of 10 kPa (ref. 35). The pressures detectable by our devices, ~50 kPa, correspond roughly to that of a firm pinch by opposing fingers. The architecture of the device, however, was not optimized.

Our devices were monolithically integrated, extremely mechanically compliant, physically robust and easily fabricated. The stretchable, transparent nanotube electrodes were prepared without dispersion in an elastic matrix, without pre-straining the substrate, and patterned simply using stencil masks. In the future, it should be possible to use these materials and principles to design organic, skin-like devices with other human—and superhuman—characteristics[36], such as the abilities to sense moisture, temperature, light[6] and chemical and biological species[37].

Methods

Preparation of substrates. PDMS (Dow Corning Sylgard 184; ratio of base to crosslinker, 10:1 by mass) was mixed, degassed and poured against the polished surface of a silicon wafer bearing either a 300 nm thermal oxide or native oxide layer. Before first use, the surfaces of the wafers were activated with oxygen plasma (150 W, 60 s, 400 mtorr) and passivated with the vapours of (tridecafluoro-1,1,2,2-tetrahydrooctyl)-1-trichlorosilane in a vacuum desiccator for ≥4 h. Curing in an oven at 60 °C for 2 h produced PDMS membranes that were ~0.3 mm thick. These membranes were cut into squares or rectangles with a razor blade with lengths and widths of 2–8 cm.

Preparation of carbon nanotube solution. Arc-discharge single-walled nanotubes (Hanwaha Nanotech Corp.) were ultrasonicated in *N*-methylpyrrolidone at 30% power for 30 min. The solution was then centrifuged for 30 min at 8,000 r.p.m. to remove large bundles, amorphous carbon or other contaminants. The top 75% of the solution was decanted for spray coating. The final solution had a concentration of ~150 μg ml^{-1}.

Spray coatings and dependence of contact angle on strain. Nanotubes were spray-coated using a commercial airbrush (Master Airbrush, Model SB844-SET). The PDMS substrates were first activated with ultraviolet/ozone for 20 min, then held at 180 °C on a hotplate, and the nanotubes were sprayed at a distance of ~10 cm using an airbrush pressure of 35 psi. We used a laser-cut PDMS membrane that had long, parallel rectangular apertures (to produce parallel lines) as a stencil mask. Multiple passes of the airbrush (>100) were performed until the desired transparency was reached. The patterned substrates were placed in a vacuum oven at 100 °C for 1 h to remove residual solvent.

We found that the surface of the ultraviolet/ozone-treated PDMS substrates became more hydrophobic with strain: when stretching from 0 to 60%, the water contact angle increased from 70 to 90°. Activation of the surface was necessary to form films in which the bundles of nanotubes were dispersed well.

Doping nanotube networks. F4TCNQ (TCI America) was dissolved to a concentration of 0.4 mmol in chloroform by bath sonication for 45 min to 1 h. The resulting bright yellow solution was filtered using a syringe filter before use. After fabrication, carbon nanotube networks were covered with sufficient solution to cover the sample surface. The solution was left to sit for 60 s, and excess was then removed by spinning at 3,000 r.p.m. for 40 s. Samples were left to air dry for at least 30 min before measuring.

Fabrication of capacitive arrays. PDMS substrates patterned with nanotubes were stretched to 25% before laminating with one another. We mixed and degassed Ecoflex 0010 silicone elastomer (Smooth-On 0010, TFB Plastics, 1:1 base to crosslinker by volume) and spread it (using a piece of PDMS membrane as a 'paintbrush') over the surface of one of the patterned substrates. We oriented a second substrate, face down, perpendicular to the first, and pressed down. We expelled air bubbles and excess Ecoflex by rolling using a roll of tape. We placed drops of EGaIn (Aldrich) on one of the two exposed termini of each line, placed a copper wire in each drop of EGaIn, and embedded the EGaIn drops with additional Ecoflex. Curing at 100 °C for 1 h produced monolithic arrays of capacitive pressure sensors.

Electrochemical, optical and sheet-resistance measurements. We measured resistance versus strain of single- and multipixel devices by clamping the device into a purpose-built, programmable stage to apply tensile strain. We measured resistance and capacitance using an LCR (inductance, capacitance, resistance) meter (Agilent E498A precision LCR meter) interfaced with a custom LabView script. We measured capacitance versus strain by applying compressive force perpendicular to the device,

with the device placed between a programmable vertically movable stage and a force gauge (Mark-10 model BG05) with a probe (area of contact defined by a square cut from a glass slide). In all cases, we used EGaIn to form deformable electrical contacts to the stretchable nanotube films.

We measured the optical transmission of the nanotube films using a Cary 6000i spectrophotometer. The reported values of transmission were taken at 550 nm.

We obtained measurements of sheet resistance using four collinear, equally spaced probes connected to a Keithley 2400 sourcemeter.

Received 7 September 2011; accepted 27 September 2011; published online 23 October 2011; corrected online 28 October 2011

References

1. LeMieux, M. C. & Bao, Z. N. Flexible electronics: stretching our imagination. *Nature Nanotech.* **3,** 585–586 (2008).
2. Kim, B. Y. S., Rutka, J. T. & Chan, W. C. W. Current concepts: nanomedicine. *New Engl. J. Med.* **363,** 2434–2443 (2010).
3. Ilievski, F., Mazzeo, A. D., Shepherd, R. F., Chen, X. & Whitesides, G. M. Soft sobotics for chemists. *Angew. Chem. Int. Ed.* **50,** 1890–1895 (2011).
4. Cotton, D. P. J., Graz, I. M. & Lacour, S. P. A multifunctional capacitive sensor for stretchable electronic skins. *IEEE Sens. J.* **9,** 2008–2009 (2009).
5. Sekitani, T. *et al.* Stretchable active-matrix organic light-emitting diode display using printable elastic conductors. *Nature Mater.* **8,** 494–499 (2009).
6. Lipomi, D. J., Tee, B. C.-K., Vosgueritchian, M. & Bao, Z. N. Stretchable organic solar cells. *Adv. Mater.* **23,** 1771–1775 (2011).
7. Ko, H. C. *et al.* A hemispherical electronic eye camera based on compressible silicon optoelectronics. *Nature* **454,** 748–753 (2008).
8. Kim, D. H. *et al.* Dissolvable films of silk fibroin for ultrathin conformal bio-integrated electronics. *Nature Mater.* **9,** 511–517 (2010).
9. Kim, R. H. *et al.* Waterproof AlInGaP optoelectronics on stretchable substrates with applications in biomedicine and robotics. *Nature Mater.* **9,** 929–937 (2010).
10. Kim, D. H. *et al.* Epidermal electronics. *Science* **333,** 838–843 (2011).
11. Viventi, J. *et al.* A conformal, bio-interfaced class of silicon electronics for mapping cardiac electrophysiology. *Sci. Transl. Med.* **2,** 24ra22 (2010).
12. Graz, I. M., Cotton, D. P. J. & Lacour, S. P. Extended cyclic uniaxial loading of stretchable gold thin-films on elastomeric substrates. *Appl. Phys. Lett.* **98,** 071902 (2009).
13. Jones, J., Lacour, S. P., Wagner, S. & Suo, Z. G. Stretchable wavy metal interconnects. *J. Vac. Sci. Technol. A* **22,** 1723–1725 (2004).
14. Tahk, D., Lee, H. H. & Khang, D. Y. Elastic moduli of organic electronic materials by the buckling method. *Macromolecules* **42,** 7079–7083 (2009).
15. Zhang, Y. Y. *et al.* Polymer-embedded carbon nanotube ribbons for stretchable conductors. *Adv. Mater.* **22,** 3027–3031 (2010).
16. Kim, K. S. *et al.* Large-scale pattern growth of graphene films for stretchable transparent electrodes. *Nature* **457,** 706–710 (2009).
17. Avouris, P. Carbon nanotube electronics and photonics. *Phys. Today* **62,** 34–40 (2009).
18. Bae, S. *et al.* Roll-to-roll production of 30-inch graphene films for transparent electrodes. *Nature Nanotech.* **5,** 574–578 (2010).
19. Feng, C. *et al.* Flexible, stretchable, transparent conducting films made from superaligned carbon nanotubes. *Adv. Funct. Mater.* **20,** 885–891 (2010).
20. Hu, L. B., Yuan, W., Brochu, P., Gruner, G. & Pei, Q. B. Highly stretchable, conductive, and transparent nanotube thin films. *Appl. Phys. Lett.* **94,** 161108 (2009).
21. Yu, Z. B., Niu, X. F., Liu, Z. & Pei, Q. B. Intrinsically stretchable polymer light-emitting devices using carbon nanotube-polymer composite electrodes. *Adv. Mater.* **23,** 3989–3994 (2011).
22. Chun, K. Y. *et al.* Highly conductive, printable and stretchable composite films of carbon nanotubes and silver. *Nature Nanotech.* **5,** 853–857 (2010).
23. Yu, C. J., Masarapu, C., Rong, J. P., Wei, B. Q. & Jiang, H. Q. Stretchable supercapacitors based on buckled single-walled carbon nanotube macrofilms. *Adv. Mater.* **21,** 4793–4797 (2009).
24. Bekyarova, E. *et al.* Electronic properties of single-walled carbon nanotube networks. *J. Am. Chem. Soc* **127,** 5990–5995 (2005).
25. Hu, L. B., Hecht, D. S. & Gruner, G. Carbon nanotube thin films: fabrication, properties, and applications. *Chem. Rev.* **110,** 5790–5844 (2010).
26. Nosho, Y., Ohno, Y., Kishimoto, S. & Mizutani, T. The effects of chemical doping with F(4)TCNQ in carbon nanotube field-effect transistors studied by the transmission-line-model technique. *Nanotechnology* **18,** 415202 (2007).
27. Khang, D. Y. *et al.* Molecular scale buckling mechanics in individual aligned single-wall carbon nanotubes on elastomeric substrates. *Nano Lett.* **8,** 124–130 (2008).
28. Kubo, M. *et al.* Stretchable microfluidic radiofrequency antennas. *Adv. Mater.* **22,** 2749–2752 (2010).
29. Cao, Q. & Rogers, J. A. Ultrathin films of single-walled carbon nanotubes for electronics and sensors: a review of fundamental and applied aspects. *Adv. Mater.* **21,** 29–53 (2009).
30. Jackman, R. J., Duffy, D. C., Cherniavskaya, O. & Whitesides, G. M. Using elastomeric membranes as dry resists and for dry lift-off. *Langmuir* **15,** 2973–2984 (1999).
31. So, J. H. *et al.* Reversibly deformable and mechanically tunable fluidic antennas. *Adv. Funct. Mater.* **19,** 3632–3637 (2009).
32. Dickey, M. D. *et al.* Eutectic gallium-indium (EGaIn): a liquid metal alloy for the formation of stable structures in microchannels at room temperature. *Adv. Funct. Mater.* **18,** 1097–1104 (2008).
33. Mannsfeld, S. C. B. *et al.* Highly sensitive flexible pressure sensors with microstructured rubber dielectric layers. *Nature Mater.* **9,** 859–864 (2010).
34. Takei, K. *et al.* Nanowire active-matrix circuitry for low-voltage macroscale artificial skin. *Nature Mater.* **9,** 821–826 (2010).
35. Someya, T. *et al.* Conformable, flexible, large-area networks of pressure and thermal sensors with organic transistor active matrixes. *Proc. Natl Acad. Sci. USA* **102,** 12321–12325 (2005).
36. Sokolov, A. N., Tee, B. C.-K., Bettinger, C. J., Tok, J. B.-H. & Bao, Z. N. Chemical and engineering approaches to enable organic field-effect transistors for electronic skin applications. *Acc. Chem. Res.* (in the press).
37. Roberts, M. E., Sokolov, A. N. & Bao, Z. N. Material and device considerations for organic thin-film transistor sensors. *J. Mater. Chem.* **19,** 3351–3363 (2009).

Acknowledgements

This work was supported by a US Intelligence Community Postdoctoral Fellowship (to D.J.L.) and the Stanford Global Climate and Energy Program. B.C-K.T. was supported by the Singapore National Science Scholarship from the Agency for Science Technology and Research (A*STAR). The authors thank V. Ballarotto for helpful discussions and J.A. Bolander for writing code for the apparatus used for electromechanical measurements.

Author contributions

D.J.L. and Z.B. conceived the project. D.J.L., M.V. and B.C-K.T. performed and designed the experiments. S.L.H. prepared the materials and developed the conditions used to dope the nanotube films. J.A.L. deposited additional nanotube films. J.A.L. and C.H.F. performed experiments on resistance versus strain. D.J.L., B.C-K.T., M.V., S.L.H. and Z.B. analysed the data. D.J.L. wrote the paper. All authors discussed the results and commented on the manuscript.

Additional information

The authors declare no competing financial interests. Supplementary information accompanies this paper at www.nature.com/naturenanotechnology. Reprints and permission information is available online at http://www.nature.com/reprints. Correspondence and requests for materials should be addressed to Z.B.